Biomechanics of Aqueous Humor Outflow Resistance*

M Johnson, Northwestern University, Evanston, IL, USA
E R Tamm, University of Regensburg, Regensburg, Germany

Glossary

Conventional aqueous outflow pathway – Comprised of the trabecular meshwork, the juxtacanalicular connective tissue, the endothelial lining of Schlemm's canal, Schlemm's canal itself, the collecting channels, and aqueous veins.
Flow resistance – The flow resistance ($R=\Delta P/Q$) of a tissue is the ratio between the pressure drop across that tissue (ΔP) and the flow rate generated by that pressure drop (Q).
Giant vacuoles – The outpouchings of the inner-wall endothelium of Schlemm's canal into its lumen. They are caused by the pressure drop across inner-wall endothelial cells.
Hydraulic conductivity (L_p) – A measure of the ease with which a fluid passes through a tissue: $L_p=Q/A/\Delta P$ where A is the cross-sectional area of the tissue facing flow.
Inner-wall region – Comprised of the inner-wall endothelium of Schlemm's canal, its basement membrane, and the adjacent juxtacanalicular tissue.
Laser trabeculoplasty – The surgical treatment of glaucoma, in which a laser beam is focused on the trabecular meshwork making tiny, evenly spaced burns.

More than 135 years ago, in 1873, Leber recognized that the elevated pressure characteristic of primary open-angle glaucoma arises due to an increased resistance to the outflow of aqueous humor out of the eye. However, a conclusive determination of where in the outflow pathways this elevated outflow resistance is generated has been elusive. Surprisingly, the locus of aqueous humor outflow resistance in the normal eye has also not been unequivocally determined.

In 1921, Seidel, using light microscopy, stated "that the inner wall of Schlemm's canal stand in open communication with the anterior chamber, and that the aqueous humor directly washes around the inner wall endothelium of Schlemm's canal and is only separated from the lumen of Schlemm's canal by a thin, outer membrane." Our view is little different today. The locus of outflow resistance, both in the normal eye and the glaucomatous eye, is thought to arise either in the endothelial lining of Schlemm's canal, or very near to this location. In this article, current viewpoints on where that flow resistance might be generated are reviewed.

There are a number of excellent review articles (see the section titled 'Further reading') that describe the detailed morphology and physiology of the aqueous outflow pathway. Here, we first review the evidence leading to the conclusion that the region surrounding the inner-wall endothelium of Schlemm's canal generates the bulk of aqueous outflow resistance. We then turn our attention to the aspect of the outflow nearest to the endothelial lining of Schlemm's canal, and examine the transport characteristics of those structures.

The bulk of the aqueous humor flows out of the anterior chamber of the eye through the conventional aqueous outflow pathway comprised of the trabecular meshwork (TM), the juxtacanalicular connective tissue, the endothelial lining of Schlemm's canal, Schlemm's canal itself, the collecting channels, and aqueous veins, and, then finally, drains into the episcleral venous system, rejoining the venous system. A second unconventional outflow pathway exists, but carries less than 10% of the total flow in the adult human eye, and thus does not significantly contribute to the dynamics of aqueous humor outflow in the normal eye. This pathway is important, however, for the understanding of the mechanism of action of prostaglandins in the treatment of glaucoma.

Regions of Low Outflow Resistance

In this section, those aspects of the conventional aqueous humor outflow pathway that are generally agreed to have small or negligible outflow resistance are examined. These include the TM, Schlemm's canal, and the collector channels and aqueous veins.

The TM is made up of the uveal meshwork, corneoscleral meshwork, and the juxtacanalicular connective tissue (JCT). The former two regions are highly porous structures with numerous openings that range in size from 25 to 75 μm in the proximal regions of the uveal meshwork to 2–15 μm in the deeper aspects of the corneoscleral meshwork. In 1958, McEwen used Poiseuille's law to show that a single pore that is 100 μm long (the thickness of the TM) and 20 μm in diameter could carry the entire aqueous humor flow with a pressure drop of 5 mmHg, and thus concluded that there was negligible flow resistance in

*Adapted from Johnson, M. (2006). What controls aqueous humour outflow resistance? *Experimental Eye Research* 82: 545–557.

this region. In 1963, Grant provided experimental support for this conclusion by cutting through the proximal aspects of the meshwork of enucleated human eyes and found no effect on outflow resistance. The JCT is discussed in the next section.

Schlemm's canal and its endothelium, shown in **Figure 1**, exist between the JCT and the sclera.

While the canal is open at low intraocular pressures (IOPs), Johnstone and Grant, in 1973, showed that the TM expands and Schlemm's canal collapses as the IOP is increased. While the size of the canal at low IOP is much too large to generate a significant outflow resistance, the collapse of Schlemm's canal at higher IOP has led some to speculate that this might be a cause of primary open-angle glaucoma. However, in 1983, Johnson and Kamm pointed out that outflow resistance, when measured at high IOP in nonglaucomatous human eyes, is not nearly as high as that of a glaucomatous eye. Collapse of the canal would make a glaucomatous condition worse, but it could not cause the glaucoma.

After traveling circumferentially in Schlemm's canal, the aqueous humor enters one of approximately 30 collecting channels that connect Schlemm's canal with the aqueous veins. The collector channels and aqueous veins have diameters that are tens of microns across. The use of Poiseuille's law leads to the conclusion that these vessels should have negligible flow resistance.

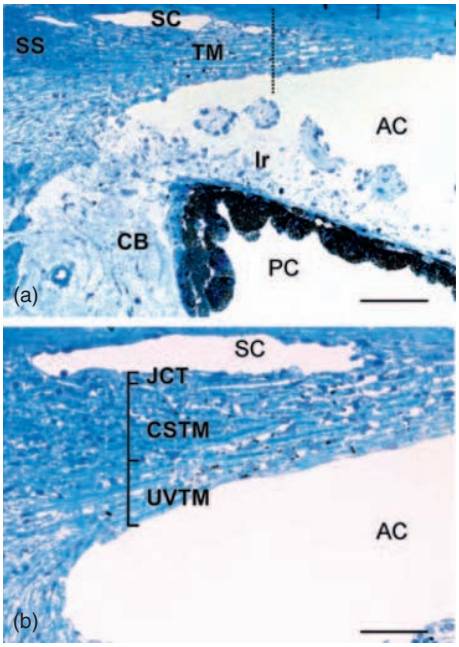

Figure 1 Light micrographs of meridional sections of the anterior chamber angle (a) and the trabecular meshwork (b). The dotted line in (a) marks the boundary between filtering and nonfiltering trabecular meshwork. SC, Schlemm's canal; TM, trabecular meshwork; SS, scleral spur; Ir, iris; CB, ciliary body; PC, posterior chamber; AC, anterior chamber; JCT, juxtacanalicular tissue; CSTM, corneoscleral trabecular meshwork; UVTM, uveal trabecular meshwork. Magnification: 100 μm (a), 50 μm (b). Adapted from Tamm, E. R. (2009). The trabecular meshwork outflow pathways. Functional morphology and surgical aspects. In: Shaarawy, T. M., Sherwood, M. B., Hitchings, R. A., and Crowston, J. G. (eds.) *Glaucoma*, vol. II, pp. 31–44. Philadelphia, PA: Saunders/Elsevier, with permission from Elsevier.

The experimental support for this conclusion is mixed. In 1992, Mäpea and Bill measured pressures in Schlemm's canal of primate eyes and found that the pressure there was little different from episcleral venous pressure. This is in agreement with the theoretical calculations. However, a 360° trabeculotomy, which would be expected to eliminate all flow resistance proximal to the collector channels and aqueous veins, leaves substantial flow resistance remaining. These disparate experimental results regarding the flow resistance of the collector channels and aqueous veins have not been reconciled, perhaps due to the fact that while a significant fraction of normal aqueous humor outflow resistance may be generated by the collector channels and/or aqueous veins, these vessels do not appear to be responsible for the elevated outflow resistance characteristic of the glaucomatous eye. Several observations lead to this conclusion. First, trabeculotomy was shown to eliminate nearly all elevated glaucomatous flow resistance in eight glaucomatous eyes. This result indicates that in primary open-angle glaucoma, the outflow obstruction is proximal to the collector channels and aqueous veins. Further support for this conclusion can be found in the success of laser trabeculoplasty (LTP) in reducing outflow resistance in glaucomatous eyes. While it is not known precisely where in the outflow pathway LTP acts, recent evidence suggests that the site of action is in the TM, and it seems very unlikely that LTP has a significant effect on the outflow resistance of the collector channels and/or aqueous veins.

The conventional wisdom now is that little, if any, significant flow resistance in the normal eye is found in the uveal meshwork, corneoscleral meshwork, Schlemm's canal, or the collector channels and aqueous veins. Furthermore, while some increased resistance might be found in these structures in the glaucomatous eye, they are not responsible for the bulk of the elevated outflow resistance characteristic of the glaucomatous eye. All evidences indicate that the bulk of normal aqueous humor outflow resistance resides in the region surrounding the inner wall of Schlemm's canal, and this is also the region where the elevated flow resistance characteristic of primary open-angle glaucoma likely arises.

The Inner-Wall Region of Schlemm's Canal

We use the term inner-wall region to refer to the inner-wall endothelium of Schlemm's canal, its basement membrane, and the adjacent JCT. **Figure 2** shows a

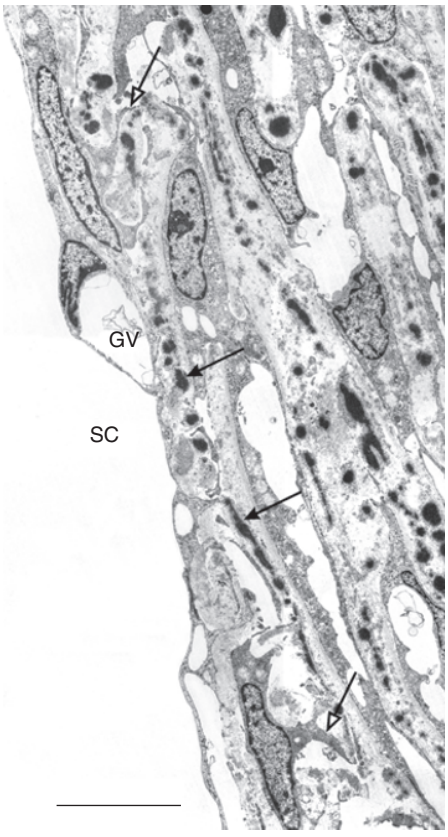

Figure 2 Electron micrograph of the inner-wall region including juxtacanalicular tissue and Schlemm's canal (SC) endothelium. The cells in the juxtacanalicular tissue form elongate processes (open arrows). Solid arrows mark the elastic fibers of the cribriform plexus. GV, giant vacuole. Magnification: 5 μm (a). Adapted from Tamm, E. R. (2009). The trabecular meshwork outflow pathways. Functional morphology and surgical aspects. In: Shaarawy, T. M., Sherwood, M. B., Hitchings, R. A., and Crowston, J. G. (eds.) *Glaucoma*, vol. II, pp. 31–44. Philadelphia, PA: Saunders/Elsevier, with permission from Elsevier.

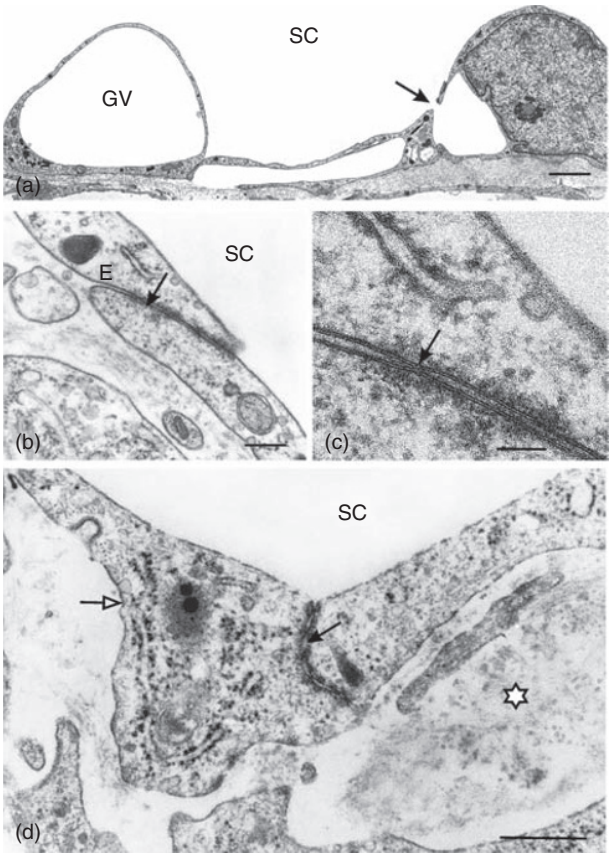

Figure 3 Electron micrographs of the endothelium of Schlemm's canal (SC) inner wall. (a) The inner-wall endothelium forms giant vacuoles (GV) in response to flow of aqueous humor. Pores (arrow) are often associated with the luminal side of the vacuoles. (b, c) Junctional complex (arrow) between two neighboring inner-wall endothelial cells; (c) is higher magnification of (b). The arrow in (c) denotes a tight junction. (d) The basal side of Schlemm's canal endothelial cells is in contact with fine fibrillar material (asterisk) and is often not covered by a basal lamina (open arrow). The solid arrow marks a junctional complex between two adjacent endothelial cells. Magnification: 2 μm (a), 250 nm (b), 125 nm (c), 500 nm (d). Adapted from Tamm, E. R. (2009). The trabecular meshwork outflow pathways. Functional morphology and surgical aspects. In: Shaarawy, T. M., Sherwood, M. B., Hitchings, R. A., and Crowston, J. G. (eds.) *Glaucoma*, vol. II, pp. 31–44. Philadelphia, PA: Saunders/Elsevier, with permission from Elsevier.

transmission electron micrograph (TEM) of the tissues that neighbors Schlemm's canal on its upstream side.

The endothelial lining of the inner wall of Schlemm's canal is typical in some ways of other vascular linings. The cells have their long axis parallel to the canal (in the direction of flow through the canal) with a length of 40–100 μm and a width of 5–15 μm. They are attached to one another with tight junctions.

This endothelium has several unique characteristics. First, structures known as giant vacuoles are seen in this layer (**Figure 3**). While they appear to be intracellular structures, giant vacuoles are really outpouchings of the endothelium into Schlemm's canal, caused by the pressure drop across inner-wall endothelial cells. In 1978, Grierson and Lee showed that these structures were invaginations into the canal with most having a large opening on the meshwork side of the vacuole and a smaller percentage (20–30%) also having a distal opening, a pore (**Figure 3**). Thus, some of the vacuoles are transcellular channels.

The distal openings, or pores, in these vacuoles are a second feature of the inner-wall endothelium that is relatively unique (**Figure 3**). Majority of these pores are transcellular, although a fraction of these pores are located at the border of two cells (border pores), and thus not transcellular but paracellular. These transcellular pores do not connect the extracellular fluid with the cytoplasm of the cell. Instead, they pass from the basal side of the cell to the apical side at a location on the cell surface where the cell membranes from the inner and outer surfaces of

the cell have come together and fused. The pore is thus membrane-lined on its surface. These pores usually form on giant vacuoles, since it is this region in which the cell is greatly attenuated and the cytoplasm becomes thin.

Fusion of the inner and outer cell membranes and the formation of transcellular pores are not entirely unique to these cells. Pores associated with giant vacuoles are also found on the arachnoid villi in the drainage pathway for the cerebrospinal fluid. When cell thickness is reduced below a critical measure, vascular endothelium can form transcellular pores involved in transport processes.

The inner-wall endothelium of Schlemm's canal is supported by a discontinuous basement membrane. This makes Schlemm's canal a somewhat unique vessel having a continuous endothelium with tight junctions between neighboring cells, supported by a discontinuous basement membrane. Blood vessel endothelia have a continuous endothelium with a continuous basement membrane, while lymphatics have a discontinuous endothelium with a discontinuous basement membrane.

The region immediately underlying the inner wall and basement membrane and extending to the last trabecular beam is the JCT. It has many large, apparently empty spaces and is typically 2–15 μm thick.

The Generation of Flow Resistance in the Inner-Wall Region of Schlemm's Canal

While there is agreement among most investigators that the bulk of aqueous humor outflow resistance is generated in the immediate vicinity of the inner-wall endothelium of Schlemm's canal, the precise location and the mechanism by which this dissipation occurs is still a topic of active debate and research.

The JCT

With its tortuous submicron-sized flow pathways, the JCT is a natural location to investigate as to its role in generating outflow resistance. Surprisingly, morphometric analyses combined with theoretical calculations have indicated that, unless these apparently open spaces are actually filled with an extracellular matrix gel, they would generate an insignificant fraction of the total outflow resistance.

This conclusion follows from porous media theory an approach that has been used to characterize flow resistance of other connective tissues. Several different parameters can be used to characterize the fluid transport capacity of a tissue. The flow resistance ($R = \Delta P/Q$) of a tissue is the ratio between the pressure drop across that tissue (ΔP) and the flow rate generated by that pressure drop (Q); the inverse of this quantity is known as the total hydraulic conductance of this tissue. The conductance per unit surface area is known as the hydraulic conductivity (L_p), while the conductance of the tissue normalized for surface area, tissue length in the flow wise direction (L), and fluid viscosity (μ) is known as the specific hydraulic conductivity (K).

Darcy's law relates the flow resistance (R) of a tissue to the specific hydraulic conductivity (K) of that tissue,

$$R = \frac{\Delta P}{Q} = \frac{\mu L}{KA} \quad [1]$$

and the specific hydraulic conductivity is related to the hydraulic conductivity as:

$$K = L_p \mu L \quad [2]$$

Typical values of K and L_p for a variety of tissues are found in **Tables 1** and **2**.

The K value that characterizes the flow resistance of a tissue can be measured experimentally by determining the other parameters in eqn [1], all of which are easy to determine or estimate for aqueous humor outflow with the exception of the length (L) over which the pressure drop occurs. However, since the bulk of the pressure drop occurs somewhere in or near the inner wall of Schlemm's canal, it can be concluded that this length is less than roughly 10 μm, or so, an estimate supported by experimental studies. Using

Table 1 Specific hydraulic conductivity (k) of connective tissues

Tissue	$K \times 10^{14}$ (cm^2)
Lens capsule[a]	0.1
Descemet's membrane[b]	0.1–0.2
Bruch's membrane[c]	0.5–1.5
Glomerulus basement membrane[d]	2
Aortic wall[e]	0.5–2.5
Corneal stroma[e]	0.5–2.5
Sclera[e]	1.4
Cartilage[f]	1–10
Synovium[g]	1.5–7
Vitreous humor[h]	1500–1800

[a]Fels, I. G. (1970). Permeability of the anterior bovine lens capsule. *Experimental Eye Research* 10: 8–14.
[b]Fatt, I. (1969). Permeability of Descemet's membrane to water. *Experimental Eye Research* 8: 34–354.
[c]Starita, C., Hussain, A. A., et al. (1997). Localization of the major site of resistance to fluid transport in Bruch's membrane. *Investigative Ophthalmology and Visual Science* 38: 762–767.
[d]Robertson, G. B. and Walton, H. A. (1989). Glomerular basement membrane as a compressible ultrafilter. *Microvascular Research* 38: 36–48.
[e]Levick, J. R. (1987). Flow through interstitium and other fibrous matrices. *Quarterly Journal of Experimental Physiology* 72: 409–437.
[f]Mow, V. C., Holmes, M. H., et al. (1984). Fluid transport and mechanical properties of articular cartilage: a review. *Journal of Biomechanics* 17: 377.
[g]Levick, J. R., Price, F. M., et al. (1996). Synovial matrix–synovial fluid system of joints. In: Comper, W. D. (ed.) *Extracellular Matrix*, vol I, pp. 328–377. Amsterdam: Harwood Academic.
[h]Fatt, I. (1977). Hydraulic flow conductivity of the vitreous gel. *Investigative Ophthalmology and Visual Science* 16: 565–568.

Table 2 Hydraulic conductivity (L_p: cm^{2*} s g^{-1}) for a variety of physiological membranes

Membrane	*Type*	$L_p \times 10^{11}$
Kidney epithelial cells (MDCK cells)	a	0.075
Xenopus oocytes[15]	a	0.2
Xenopus oocytes + CHIP28[15]	a	1.6
Proximal tubule epithelial cells[1,2]	a	1.2
Red blood cells[12,14]	a	1–1.6
Gall bladder epithelial cells[13]	a	4–9
Corneal epithelium[2,9]	b	0.04–0.7
Gall bladder epithelium[12,13]	b	1.3–3.6
Proximal tubule epithelium[1,12]	b	7.5–5.5
Retinal pigment epithelium[3]	b	16
Brain capillary[4]	c	0.03
Corneal endothelium[2,5]	c	0.14–5
Lung capillary[4]	c	3.4
Skeletal muscle capillary[4,7]	c	2.5–7
Cardiac muscle capillary[4,7]	c	8.6
Aorta[6]	c	9
Mesentery, omentum[4]	c	50
Intestinal mucosa[4,7]	d	32–130
Synovium (knee)[7]	d	120
Renal peritubulal capillaries[7]	d	225–700
Renal glomerulus[4,7]	d	400–3100
Descemet's membrane[9]	e	15–37
Lens capsule[10]	e	17–50
Bruch's membrane[11]	e	2000–12,500
Kidney tubule basement membrane[8]	e	6300–13,700

a: cell membranes, b: unfenestrated epithelium, c: unfenestrated endothelium, d: fenestrated epithelia, and e: basement membranes.

[1]Timbs, M. M. and Spring, K. R. (1996). Hydraulic properties of MDCK cell epithelium. *Journal of Membrane Biology* 153: 1–11.
[2]Klyce, S. D. and Russell, S. R. (1979). Numerical solution of coupled transport equations applied to corneal hydration dynamics. *Journal of Physiology* 292: 107–134.
[3]Tsuboi, S. (1987). Measurement of the volume flow and hydraulic conductivity across the isolated dog retinal pigment epithelium. *Investigative Ophthalmology and Visual Science* 28: 1776–1782.
[4]Renkin, E. M. (1977). Multiple pathways of capillary permeability. *Circulation Research* 41: 735–743.
[5]Hedbys, B. O. and Mishima, S. (1962). Flow of water in corneal stroma. *Experimental Eye Research* 1: 262–275.
[6]Vargas, C. B., Vargas, F. F., et al. (1979). Hydraulic conductivity of the endothelial and outer layers of rabbit aorta. *American Journal of Physiology* 236: H53–H60.
[7]Levick, J. R. (1987). Flow through interstitium and other fibrous matrices. *Quarterly Journal of Experimental Physiology* 72: 409–437.
[8]Welling, L. and Welling, D. (1978). Physical properties of isolated perfused basement membranes from rabbit loop of Henle. American *Journal of Physiology* 234: F54–F58.
[9]Fatt, I. (1969). Permeability of Descemet's membrane to water. *Experimental Eye Research* 8: 34–354.
[10]Fisher, R. F. (1982). The water permeability of basement membrane under increasing pressure: evidence for a new theory of permeability. *Proceedings of the Royal Society of London Series* B 216: 475–496.
[11]Starita, C., Hussain, A., et al. (1996). Hydrodynamics of ageing Bruch's membrane: implications for macular disease. *Experimental Eye Research* 62: 565–572; Bentzel, C. and Reczek, P. (1978). Permeability changes in Necturus proximal tubule during volume expansion. *American Journal of Physiology* 234: F225–F234.
[12]Gonzalez, E., Carpi-Medina, P., et al. (1982). Cell osmotic water permeability of isolated rabbit proximal straight tubules. *American Journal of Ophthalmology* 242: F321–F330.
[13]Persson, B. E. and Spring, K. R. (1982). Gallbladder epithelial cell hydraulic water permeability and volume regulation. *Journal of General Physiology* 79: 481–505.
[14]Solomon, A. K., Chasan, B., et al. (1983). The aqueous pore in the red cell membrane: band 3 as a channel for anions, cations, nonelectrolytes, and water. *Annals of the New York Academy of Sciences* 414: 97–124.
[15]Preston, G. M., Carroll, T. P., et al. (1992). Appearance of water channels in Xenopus oocytes expressing red cell CHIP28 protein. *Science* 256: 385–387.

a flow rate through the aqueous outflow pathway of 2 μl min^{-1} passing through a cross-sectional area of between 0.054 and 0.13 cm^2 (canal width of 150–350 μm; canal length around the eye of 3.6 cm), and a pressure drop of 5 mmHg, it can then determined that K of the resistance-causing region in the aqueous outflow pathway must be less than 65×10^{-14} cm^2. Unless the length over with the pressure drop occurs (L) is much lesser than 10 μm, the specific hydraulic conductivity of the connective tissue elements in the outflow pathway is greater than that of any other connective tissue with the exception of the vitreous humor (**Table 1**).

K can also be estimated from photomicrographs showing the ultrastructure of a tissue. This can potentially allow an evaluation of which structures in the aqueous outflow pathway are generating the measured outflow resistance. Carmen–Kozeny theory relates the structure of a porous medium to K as:

$$K = \frac{\varepsilon \, D_h^2}{80} \qquad [3]$$

where D_h is the hydraulic diameter of the open spaces available for flow and ε is the porosity, or fraction of open space of the medium (note that at porosities higher than roughly 0.8, this equation becomes inaccurate). Using Carmen–Kozeny theory combined with conventional TEM, it was found (in immersion-fixed eyes) that the porosity of the JCT was approximately 0.15–0.25, D_h was approximately 1–1.5 μm, and, most importantly, K of the JCT was calculated to be approximately 2000–10 000 10^{-14} cm^2 based on the photomicrographs. This is, at least, 30 times greater than K based upon measured properties of the outflow system.

In 1986, Ethier and coworkers concluded that the JCT, as visualized using conventional TEM, could not generate a significant fraction of outflow resistance. Other investigators have confirmed this conclusion, including studies in which the eyes were fixed by perfusion. It thus followed that either this region was filled with an extracellular matrix gel that was poorly visualized using

conventional TEM techniques, or, that this region was not the primary site of outflow resistance. The age-related accumulation of plaque-like material in this region that is reported to be enhanced in glaucomatous eyes would have no influence on this conclusion.

More recently, in 2002, Gong and coworkers used quick-freeze/deep-etch (QFDE) methodology to examine the apparent open spaces seen in the JCT region in greater detail. QFDE is a morphological technique that preserves the cellular and extracellular ultrastructure in exquisite detail and allows visualization of structures poorly preserved or not seen at all using conventional TEM tissue preparation techniques. A more elaborate and extensive extracellular matrix was seen in the JCT using QFDE as compared to conventional methods of preparation for TEM (**Figure 4**); however, micron-sized open spaces were still seen in this region, casting doubt on whether a significant fraction of outflow resistance could be generated in this region. An important caveat pointed out by the Gong group regarding their studies was that it was not clear whether or not QFDE can visualize the glycosaminoglycans (GAGs) in their uncollapsed state, and this leaves uncertain the question of generation of appreciable flow resistance in the JCT region.

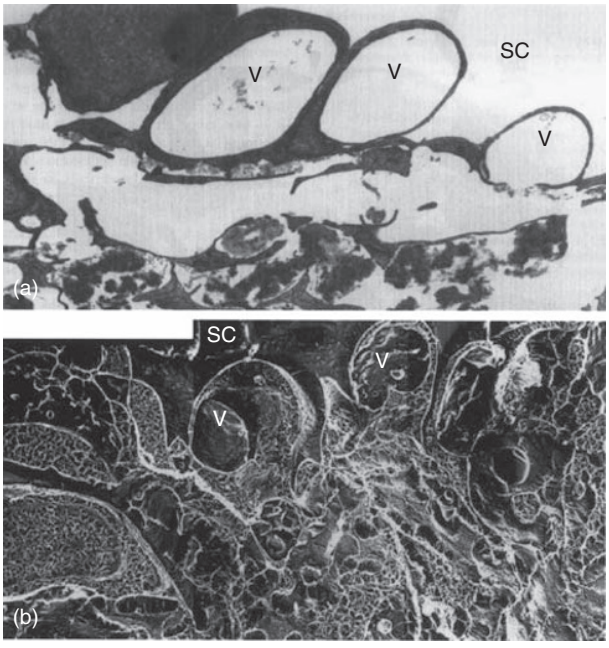

Figure 4 Enucleated human eye fixed by perfusion at 15 mmHg: (5A) vacuoles (V) in the inner wall of Schlemm's canal (SC) in tissue prepared for TEM using conventional methods; notice the large open space in the region of the JCT immediately under these vacuoles; (4B) the same region as seen in tissue prepared using QFDE; notice that while open spaces still exist under the vacuoles, a more complex and extensive extracellular matrix is seen. Magnification ×4860. Adapted from Gong, H., Ruberti, J., Overby, D., Johnson, M., and Freddo, T. F. (2002). A new view of the human trabecular meshwork using quick-freeze, deep-etch electron microscopy. *Experimental Eye Research* 75: 347–358, with permission from Elsevier.

The role that GAGs and other extracellular matrix elements found in the JCT might play in generating outflow resistance is unclear. While it has been shown that enzymes that degrade macromolecules (GAGases) increase outflow facility in a number of species (e.g., cow, guinea pig, dog, and rabbit), the evidence regarding primates is conflicting, and there has been no confirmed data yet showing that GAGases decrease outflow resistance in human eyes. Matrix metalloproteinases (MMPs) have been shown to reversibly increase outflow facility in perfused human anterior segment organ culture, and this is a strong indicator that the extracellular matrix may generate significant aqueous outflow resistance.

Perhaps the strongest experimental evidence implicating the JCT as a major site of outflow resistance is the 1992 study by Maepea and Bill in which they used micropipettes and localized the pressure drop to occurring somewhere between 7 and 14 μm from the inner wall of Schlemm's canal (i.e., in the JCT). While this result is frequently cited in the literature, it is not widely appreciated that this measurement was made with micropipettes whose tip sizes were as large as the measurement zone. When this reservation is combined with the fact that the inner wall of Schlemm's canal distends several to many microns during the process of penetration by the micropressure probe (unpublished work by Dr. Milko Iliev in collaboration with Dr. Johnson's laboratory), it leads to the conclusion that the bulk of the aqueous humor pressure drop occurs near the inner wall of Schlemm's canal (within 5–10 μm), but that no further quantitative conclusions are possible.

The basement membrane

The basement membrane of the inner wall of Schlemm's canal is another possible location for generation of outflow resistance. **Table 1** shows that the specific hydraulic conductivities of basement membranes (top four tissues in table) are among the lowest of connective tissues.

However, basement membranes tend to be quite thin and this limits the flow resistance they can generate (see eqn [1]). **Table 2** shows the hydraulic conductivity of a variety of physiological membranes, including cells membranes, epithelia, and basement membranes. The large variation in L_p of basement membranes is due not only to variation in the specific hydraulic conductivity of these tissues, but also to significant differences in their thicknesses (ranging from 0.15 μm for Bruch's membrane to 7 μm for Descemet's membrane).

It is interesting to compare the values seen in this table with the estimated value of the hydraulic conductivity of the outflow pathway. From the definition of hydraulic conductivity (or by combining eqns [1] and [2]), $L_p = Q / A/\Delta P$. Using the values characterizing the aqueous

outflow pathway presented above, we can estimate that L_p for the aqueous humor outflow pathway is between 4000 $\times 10^{-11}$ and 9000 $\times 10^{-11}$ cm^2 s g^{-1}. Note that this is not a theoretical calculation but an estimate based on measured quantities.

Table 2 shows that several basement membranes, in particular those of the renal system, have hydraulic conductivities similar to that of the aqueous outflow pathway. This suggests that the basement membrane of the inner-wall endothelium of Schlemm's canal might be an important contributor to aqueous humor outflow resistance.

However, as noted above, this basement membrane is discontinuous (**Figure 3**), as recently confirmed in 2002 by Gong and coworkers. If there are breaks in the basement membrane, it is difficult to see how a significant flow resistance could be generated by this tissue.

The inner-wall endothelium of Schlemm's canal

The inner-wall endothelium of Schlemm's canal has been an attractive candidate for the generation of outflow resistance since the time that light microscopes and later electron microscopes were focused on the inner-wall endothelium. Comparison of the hydraulic conductivity of this tissue (4000–9000 $\times 10^{-11}$ cm^2 s g^{-1}) with that of other endothelia and epithelia as seen in **Table 2**, leads one to conclude that this vessel lining must have one of the highest hydraulic conductivities in the body. Compared to other tissues in **Table 2**, it is clear that only fenestrated endothelia (and some basement membranes) have such high hydraulic conductivities.

While the inner-wall endothelium is not fenestrated, this endothelium is unique in that it contains micron-sized pores. It is interesting that even early investigators (e.g., Seidel) had concluded that such pores existed, long before they were first seen by electron microscopy. This conclusion was based on early filtration studies that examined the sizes of microparticulates that would pass through the outflow pathway. It was found in these studies that a filtration barrier existed for particles larger than roughly 0.5 μm or so, and thus it was concluded that pores nearly 1 μm in size must exist. More recent studies have confirmed this conclusion using microparticles and latex microspheres.

While there is some debate concerning the existence of these pores (which is discussed below), no group has offered an alternate explanation for the extraordinarily high hydraulic conductivity of the aqueous outflow pathway. Nor has any alternate explanation been offered for the relatively easy passage of microparticles 200–500 nm in diameter through the outflow pathway, except through these large pores. Since there are tight junctions (**Figure 3**) between the inner-wall cells (presumably to prevent blood reflux into the eye that can occur during periods of transient increases in ocular venous pressure), there are no other structures apparent in this endothelium that could explain the high hydraulic conductivity of this tissue or its filtration characteristics.

The flow resistance generated by these pores was first considered by Bill and Svedbergh in 1972. In an exhaustive study using scanning electron microscopy, they characterized the size distribution of these pores, and then used hydrodynamic theory to calculate for hydraulic conductivity of these pores. Using Sampson's law, that gives the hydraulic conductivity for a single pore of diameter d,

$$L_p = \frac{d}{6\pi\mu} \qquad [4]$$

they found that the inner-wall endothelium could present, at most, 10% of the outflow resistance. That is, the hydraulic conductivity of the pores in the inner-wall endothelium is, at least, 10-fold higher than the measured hydraulic conductivity of the outflow pathway. This conclusion has been confirmed in a number of studies.

These results would appear to rule out the inner-wall endothelium as a major site of outflow resistance. However, a number of experimental findings are at variance with this conclusion. In particular, when chelating agents (ethylenediaminetetraacetic acid (EDTA) and ethylene glycol tetraacetic acid (EGTA)) or a proteolytic enzyme (α-chymotrypsin) were perfused through the outflow pathway of live primates, it was found that ruptures of the inner-wall endothelium were produced by these agents that decreased outflow resistance more than could be explained by the calculated flow resistance of the inner-wall pores. A hydrodynamic interaction (the funneling effect) between the inner-wall pores and the JCT, which lies immediately below these pores, has been proposed as an explanation of the findings (see **Figure 5**).

In this scenario, the pores and vacuoles themselves contribute negligible flow resistance, but since they force aqueous humor to funnel through those regions of the JCT nearest the pores and vacuoles, the vacuole size

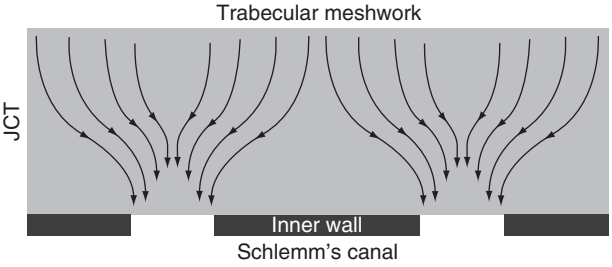

Figure 5 Schematic of the funneling of aqueous humor through the JCT, toward a vacuole and pore that allows this fluid to pass through the inner-wall endothelium. Adapted from Overby, D., Gong, H., Qiu, G., Freddo, T. F., and Johnson, M. (2002). The mechanism of increasing outflow facility during washout in the bovine eye. *Investigative Ophthalmology and Visual Science* 43: 3455–3464. ©The Association for Research in Vision and Ophthalmology.

and pore density can have a significant effect on the effective hydraulic conductivity (L_p) of the JCT:

$$L_p = \frac{2KnD}{\mu} \quad [5]$$

Here, K is the specific hydraulic conductivity of the JCT region, n is the number of pores per unit area in the inner wall, D is the diameter of the vacuoles in the inner wall, and μ is the viscosity of the aqueous humor.

The funneling model suggests that while the bulk of outflow resistance is actually generated in the JCT or basement membrane, its magnitude is modulated by the pores and vacuoles of the inner-wall endothelium of Schlemm's canal. This model explains many of the characteristics of the outflow pathways discussed above. However, two recent studies failed to find a correlation between outflow facility and inner-wall pore density as would be expected if eqn [5] describes the hydraulic conductivity of the outflow pathway. Furthermore, these studies found that at least some inner-wall pores may be artifacts of the fixation process.

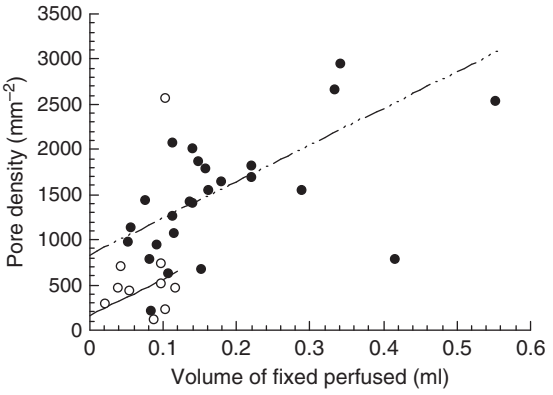

Figure 6 Pore density as a function of volume of fixative perfused through the outflow pathway of normal eyes (filled symbols) and eyes with POAG (open). Lines are best fit with outliers excluded. Adapted from Johnson, M., Chan, D., Read, A. T., et al. (2002). Glaucomatous eyes have a reduced pore density in the inner wall endothelium of Schlemm's canal. *Investigative Ophthalmology and Visual Science* 43: 2950–2955. ©The Association for Research in Vision and Ophthalmology.

Pores as possible fixation artifacts and the possible importance of flow through inner-wall cell junctions or through water channels

The micron-sized pores that pass through the endothelial cells of the inner-wall endothelium of Schlemm's canal are relatively unique to these cells and to the cells of the arachnoid villi, a tissue of the cerebrospinal fluid pathway. This unique character has led some investigators to doubt that these are physiologic structures, but instead consider them to be artifacts of the tissue-preparation process. The possibility that pores form during tissue preparation for electron microscopy was supported in recent studies that showed that during tissue fixation under flow conditions, the inner-wall endothelium pore density increased as a function of the volume of fixative perfused through the outflow pathway (see **Figure 6**).

It has been postulated by several investigators that instead of passing through the pores in the inner-wall endothelium, a significant fraction of the aqueous humor passes through gaps between the tight-junction strands of these cells. In 2001, Ethier and Chan found that cationized ferritin perfused into enucleated human eyes acted to decreased outflow facility and was seen accumulating in junctions between inner-wall endothelial cells. While Ethier and Chan argue that the decreased outflow facility caused by cationized ferritin was due to pore blocking that was also seen to occur in this study, others have interpreted their results as consistent with a significant flow through the junctional complexes.

There are a several reasons why this hypothesis is untenable. Two strong arguments against this possibility were suggested above, namely that the uniquely high hydraulic conductivity of the aqueous outflow pathway is inconsistent with flow through junctions, and that the relatively free passage of microspheres 200–500 nm in diameter through the outflow pathway would be precluded if transport was primarily through cell junctions. It is well known in the vascular system that macromolecules larger than roughly 10–20 nm are largely excluded from passing through cell junctions, for either fenestrated or nonfenestrated vessels.

In 1981, Raviola and Raviola examined the tight junctions of the inner-wall endothelium and calculated the flow that would be expected through these junctions. The gaps they found available for transport around the tight-junctional strands were nanometers in size, and they concluded that any flow that might occur through these spaces would be negligible. In 1997, Ye and coworkers used freeze-fracture techniques to examine these junctions in eyes fixed under flow conditions and did not report significant differences from the dimensions reported by Raviola and Raviola. The notion that microparticles that are roughly 0.5 μm in size could relatively easily pass through such openings seems improbable, at best.

The study of Ye and coworkers did find that the tight junctions of the inner-wall cells simplified with increasing IOP. They speculated that the junctional simplification that occurred with increasing perfusion pressure might lead to formation of pores at locations of focal separation in the tight junctions. While they did not find a statistically significant relationship between junctional complexity and outflow facility in this small series of eyes, they did find a trend in that direction, consistent with their hypothesis.

Thus, while there are a number of strong arguments against the possibility of transport of a significant quantity of aqueous humor across the inner wall of Schlemm's canal passing directly through cell junctions, simplification of these junctions might be involved in the process of pores formation. In particular, paracellular flow through border pores could be consistent with the 1991 findings of Epstein and Rohen of dilations of this paracellular space.

It has also been suggested that a fraction of outflow might pass through water channels (aquaporins) in the cell membrane of the inner-wall cells. Red blood cells and renal proximal tubules are cell types expressing high levels of aquaporin 1. The hydraulic conductivities of the water channels in these cell membranes have been measured, as have those of cells in which aquaporins are overexpressed (see **Table 2**). All of these values are more than 1000 times smaller than the hydraulic conductivity of aqueous outflow pathway. It goes without saying that water channels also cannot explain the relatively free passage of 0.5-μm-sized particles through the outflow pathway.

The only pathway that appears consistent with the available physiologic evidence is through the inner-wall pores whose existence was already postulated more than 80 years ago by Seidel in 1921, and that now are easily seen using scanning electron microscopy of this tissue. Importantly, the size of these pores is consistent with the predictions of Seidel. Whether this transport is primarily through border pores or is also through the transcellular pores remains to be determined.

The question remains as to why the number of these pores increases during the fixation process, as shown in **Figure 6**. A further finding of the studies was that the number density of pores in the inner-wall endothelium decreases as a function of postmortem time, something not expected of an artifact. Instead, it may be that fixation under flow conditions generates stresses in the inner wall due both to pressure-induced stretching of the inner wall of Schlemm's canal and also to shrinkage of the tissue following fixation. Pressure-induced stress is likely what causes the formation of these pores under physiologic conditions. Then, fixative-induced pore formation might be an artifact associated with a physiological process, namely stress on the inner-wall endothelium.

In this scenario, the y-intercepts of the lines seen on **Figure 6** would then represent the true physiological pore density of normal and glaucomatous eyes, respectively. Importantly, **Figure 6** shows this density to be greatly reduced in glaucomatous eyes. Through their importance to funneling (eqn [5]), a decrease of inner-wall pores would be expected to decrease the hydraulic conductivity of the outflow pathway and thereby increase IOP.

This decrease pore density in the inner-wall endothelium of Schlemm's canal may then represent the cause of the elevated pressure characteristic of glaucoma. Future work may then indicate why this pore density is decreased.

See also: Biological Properties of the Trabecular Meshwork Cells; The Biology of Schlemm's Canal; The Cytoskeletal Network of the Trabecular Meshwork; The Fibrillar Extracellular Matrix of the Trabecular Meshwork; Functional Morphology of the Trabecular Meshwork; Primary Open-Angle Glaucoma; Role of Proteoglycans in the Trabecular Meshwork; Structural Changes in the Trabecular Meshwork with Primary Open Angle Glaucoma; Uveoscleral Outflow.

Further Reading

Bill, A. (1975). Blood circulation and fluid dynamics in the eye. *Physiological Reviews* 55: 383–416.

Bill, A. and Mäepea, O. (1994). Mechanisms and routes of aqueous humor drainage. In: Albert, D. M. and Jakobiac, F. A. (eds.) *Principles and Practice of Ophthalmology. Vol I: Basic Sciences*, ch. 12, pp. 2577–2595. Philadelphia, PA: Saunders.

Bill, A. and Svedbergh, B. (1972). Scanning electron microscopic studies of the trabecular meshwork and the canal of Schlemm – an attempt to localize the main resistance to outflow of aqueous humor in man. *Acta Ophthamologica* 50: 295–320.

Epstein, D. L. and Rohen, J. W. (1991). Morphology of the trabecular meshwork and inner-wall endothelium after cationized ferritin perfusion in the monkey eye. *Investigative Ophthalmology and Visual Science* 32(1): 160–171.

Ethier, C. R. (2002). The inner wall of Schlemm's canal (review). *Experimental Eye Research* 74: 161–172.

Ethier, C. R., Coloma, F. M., Sit, A. J., and Johnson, M. (1998). Two pore types in the inner wall endothelium of Schlemm's canal. *Investigative Ophthalmology and Visual Science* 39: 2041–2048.

Ethier, C. R., Kamm, R. D., Palaszewski, B. A., Johnson, M. C., and Richardson, T. M. (1986). Calculations of flow resistance in the juxtacanalicular meshwork. *Investigative Ophthalmology and Visual Science* 27(12): 1741–1750.

Gong, H., Ruberti, J., Overby, D., Johnson, M., and Freddo, T. F. (2002). A new view of the human trabecular meshwork using quick-freeze, deep-etch electron microscopy. *Experimental Eye Research* 75: 347–358.

Gong, H., Tripathi, R. C., and Tripathi, B. J. (1996). Morphology of the aqueous outflow pathway. *Microscopy Research and Technique* 33: 336–367.

Grant, W. M. (1963). Experimental aqueous perfusion in enucleated human eyes. *Archives of Ophthalmology* 69: 783–801.

Johnson, M. (2006). What controls aqueous humour outflow resistance? *Experimental Eye Research* 82: 545–557.

Johnson, M. and Erickson, K. (2000). Mechanisms and routes of aqueous humor drainage. In: Albert, D. M. and Jakobiec, F. A. (eds.) *Principles and Practice of Ophthalmology. Vol. 4: Glaucoma*, ch. 193B, pp. 2577–2595. Philadelphia, PA: WB Saunders.

Johnstone, M. A. and Grant, W. M. (1973). Pressure dependent changes in the structures of the aqueous outflow system of human and monkey eyes. *American Journal of Ophthalmology* 75: 365.

Leber, T. (1873). Studien über den Flüssigkeitswechsel im Auge. *(Albrecht von Graefes) Archiv für Ophthalmologie* 19: 87–106.

Maepea, O. and Bill, A. (1992). Pressures in the juxtacanalicular tissue and Schlemm's canal in monkeys. *Experimental Eye Research* 54(6): 879–883.

Raviola, G. and Raviola, E. (1981). Paracellular route of aqueous outflow in the trabecular meshwork and canal of Schlemm. *Investigative Ophthalmology and Visual Science* 21: 52–72.

Seidel, E. (1921). Weitere experimentelle Untersuchungen über die Quelle und den Verlauf der intraokularen Saftströmung. IX Mitteilung. Über den Abfluss des Kammerwassers aus der vorderen AugenKammer. *Graefe's Archive for Clinical and Experimental Ophthalmology* 104: 357–402.

Tamm, E. R. (2009). *The trabecular meshwork outflow pathways. Functional morphology and surgical aspects*. In: Shaarawy, T. M., Sherwood, M. B., Hitchings, R. A., and Crowston, J. G. (eds.) *Glaucoma,* vol. II, pp. 31–44. Philadelphia, PA: Saunders/Elsevier.

Tripathi, R. C. (1974). Comparative physiology and anatomy of the aqueous outflow pathway. In: Davson, H. and Graham, L. T. (eds.) *The Eye. Comparative Physiology,* vol. 5, ch. 3, pp. 163–356. London: Academic Press.

Ye, W., Gong, H., Sit, A., Johnson, M., and Freddo, T. F. (1997). Interendothelial junctions in normal human Schlemm's canal respond to changes in pressure. *Investigative Ophthalmology and Visual Science* 38(12): 2460–2468.